Heliyon 10 (2024) e32814

Contents lists available at ScienceDirect

Heliyon

journal homepage: www.cell.com/heliyon

Research article

Development of a genetically encoded NMT indicator for detection of mercury ions based on the green fluorescent protein mNeonGreen and metallothionein II from rat liver

Oksana M. Subach [a], Kiryl D. Piatkevich [b,c,d], Fedor V. Subach [a,*]

[a] Complex of NBICS Technologies, National Research Center "Kurchatov Institute", Moscow, 123182, Russia
[b] School of Life Sciences, Westlake University, Hangzhou, 310024, China
[c] Westlake Laboratory of Life Sciences and Biomedicine, Hangzhou, 310024, China
[d] Institute of Basic Medical Sciences, Westlake Institute for Advanced Study, Hangzhou, 310024, China

ARTICLE INFO

Keywords:
Genetically encoded mercury indicator
Heavy metals
Green fluorescent NMT indicator
Metallothionein
Fluorescence response

ABSTRACT

Heavy metals, particularly mercury, rank as some of the most hazardous systemic toxicants known to cause multiple organ damage, even at lower levels of exposure. Its detection in the environment and in the live cells is an actual task. Here, we engineered a novel genetically encoded fluorescent NMT indicator for mercury ions by inserting the metallothionein II domain from rat liver into the bright green-yellow fluorescent protein mNeonGreen, followed by directed molecular evolution of the resulting sensor prototype in bacteria. In solution, the NMT indicator was 1.7-fold brighter than the standard eGFP fluorescent protein and responded to the addition of even 10^{-18}-10^{-19} M mercury ions by quenching fluorescence with a 5-fold fluorescence response and extremely high affinity to mercury ions characterized by the K_d value of 0.50 ± 0.05 aM. We also characterized the selectivity of the NMT indicator to other metal cations. In cultured mammalian cells, the NMT indicator detected even an extracellular concentration of 0.1 fM mercury ions and achieved a 5.9-fold change in ΔF/F fluorescence intensity.

1. Introduction

Heavy metal ions are one of the most serious contributors to environmental pollution because they are highly toxic and non-degradable substances that tend to accumulate in living organisms [1]. By definition, heavy metals (HM) are chemical elements with atomic numbers greater than 20 and atomic density greater than 5 g cm^{-3}, and they also exhibit typical metallic properties [2]. Heavy metals can be divided into two categories: essential and nonessential [3]. Essential heavy metals are necessary for living organisms to carry out fundamental biological processes such as growth, metabolism, and development of various organs. Copper (Cu^{+}/Cu^{2+}), iron (Fe^{2+}), manganese (Mn^{2+}/Mn^{3+}/Mn^{4+}), cobalt (Co^{2+}), zinc (Zn^{2+}), and nickel (Ni^{2+}) ions are classified as essential heavy metals due to their vital roles in biological organisms, such as coordinating cofactors that are structurally and functionally important to enzymes and other proteins. Nonessential heavy metals such as mercury (Hg^{2+}), cadmium (Cd^{2+}), lead (Pb^{2+}), and chromium (Cr^{3+}) ions are not required by living organisms, even in trace amounts for any of the metabolic processes. These metals, together with the semi-metal arsenic (As in the oxidation states III and V), are among the most toxic metals, as exposure to even small

* Corresponding author.
E-mail addresses: subach_om@nrcki.ru (O.M. Subach), kiryl.piatkevich@westlake.edu.cn (K.D. Piatkevich), subach_fv@nrcki.ru (F.V. Subach).

https://doi.org/10.1016/j.heliyon.2024.e32814
Received 14 April 2024; Received in revised form 7 June 2024; Accepted 10 June 2024
Available online 11 June 2024

amounts of these metals in concentrations such as 10^{-9}-10^{-10} M can cause cancer, as well as gastrointestinal, respiratory, cardiovascular, reproductive, renal, hematopoietic and neurological disorders in humans [4]. Consequently, the detection of heavy metal ions in the environment and in the cells of living organisms is a very urgent task.

Genetically encoded sensors based on fluorescent proteins are used for detection of heavy metal ions both in living cells and in various solutions. However, genetically encoded sensors for lead and chromium ions have not been developed so far. The FRET indicator SenALiB (Sensor for Arsenic Linked Blackfoot disease), containing arsenic-binding protein (ArsR) as an As^{3+} sensing element inserted between a FRET pair of cyan (ECFP) and yellow (Venus) fluorescent proteins (FPs), detected up to 11 % change in the FRET ratio at 540/485 nm upon binding by As^{3+}in live HEK cells [5]. A FRET indicator Cd-FRET-2 for Cd^{2+} ions with a fluorescence response of 30 % was also constructed, in which four cysteine residues that could form a tetrahedral metal binding site (Cys)4 were introduced at the dimerization interface of two Citrine and Cerulean FPs [6]. Two sensors for the detection of Hg^{2+} ions engineered based on eGFP [7] and IFP [8] were previously reported. The eGFP205C indicator, which features a single 205C mutation, exhibited a 30–40 % reduction in fluorescence in response to the addition of Hg^{2+} ions, with a detection threshold for mercury as low as approximately 2 nM [7]. However, its practical use has been demonstrated solely in *E. coli* cells. The infrared fluorescent protein IFP responded by quenching fluorescence to the addition of Hg^{2+} ions with the detection limit in vitro of less than 50 nM, but the disadvantage of such an indicator was that mercury ions compete with biliverdin for binding to IFP as well as interference from other free thiol-containing compounds, such as glutathione [8]. Such indicator reacted to mercury ions upon sequential addition of mercury ions and biliverdin or their simultaneous addition, but not in the state previously bound to biliverdin.

In the present work, we engineered a genetically encoded fluorescent indicator for mercury ions (Hg^{2+}), named the NMT indicator, by inserting the metallothionein II domain from rat liver into the bright green-yellow fluorescent protein mNeonGreen followed by several rounds of directed molecular evolution. Upon exposure to mercury ions, the NMT indicator exhibited fluorescence quenching with a 5-fold response in solution and a 5.9-fold response in the cytosol of HeLa cells. In mammalian cells, it was possible to detect mercury ion concentrations as low as 1 fM. The NMT indicator also responded to cadmium ions, showing a 1.5-fold fluorescence quenching, albeit with significantly lower affinity. Furthermore, we systematically characterized the specificity of the NMT indicator towards various metal ions, including heavy metals.

2. Methods

2.1. Synthesis of the metallothionein II alpha-domain gene, molecular cloning, and library preparation

The metallothionein II alpha-domain gene was synthesized *de novo* by polymerase chain reaction (PCR) with overlapping primers (Table S1). The gene was cloned at the *Bgl*II/*Eco*RI restriction sites into the pBAD/HisB plasmid and transformed into Mach1 cells. Libraries with randomized linkers were obtained by overlapping fragment PCR [9] using primers (Table S1). Libraries were cloned at *Bgl*II/*Eco*RI restriction sites into pBAD/HisB plasmid and transformed into BW25113 cells.

Random libraries were obtained by PCR in the presence of manganese ions under conditions of 2–3 mutations per 1000 base pairs. The libraries were cloned at *Bgl*II/*Eco*RI restriction sites into pBAD/HisB plasmid and transformed into BW25113 cells.

2.2. Screening of libraries

Bacterial libraries were first analyzed on Petri dishes under a Leica fluorescence stereomicroscope. Green fluorescence was acquired using excitation at 480/40 nm and emission at 535/40 nm filters. The brightest colonies were selected for further expression in liquid media and assessment of crude bacterial lysates. Respectively, selected colonies were inoculated with 5 ml of LB medium containing ampicillin (100 μg/mL) and protein expression inducer arabinose (0.004 %) and grown overnight at 37 °C with continuous shaking at 220 rpm. Cells were precipitated at 3500 rpm for 12 min, the precipitate was frozen, and 150 μl of B-Per extraction reagent containing lysozyme (1 μg/mL) and benzonase (1.25 units/mL) was added. We incubated mixtures at 37°C for 20 min at 220 rpm. The cell lysate was separated from the cells by centrifugation at 20000*g* for 2 min. Then, for each clone we prepared 200 μl of buffer A (50 mM Tris-HCl, 100 mM NaCl, 100 mM NaCl, 1 mM MgCl2, 10 mM NTA, pH 7.2) and 200 μl of buffer B (50 mM Tris-HCl, 100 mM NaCl, 1 mM MgCl2, 10 mM Hg-NTA, pH 7. 2) and recorded green fluorescence (Ex 490 and Em 510–570 nm) on a plate reader (background fluorescence). Then, 10 μl of lysate was added into a 96-well plate in 200 μl of buffer A and 200 μl of buffer B, and green fluorescence (Ex 490 and Em 510–570 nm) was recorded on a plate reader. The ΔF/F values were calculated using the formula $\Delta F/F = -[(I_{NTA}\text{-}I_{back1})/(I_{Hg\text{-}NTA}\text{-}I_{back2})\text{-}1]$.

2.3. Purification and characterization of proteins in vitro

To characterize the spectral properties in vitro, proteins were purified from 250 ml of LB medium containing ampicillin (100 μg/ml) and protein expression inducer arabinose (0.004 %) and grown overnight at 37°C, 220 rpm. Cells were precipitated at 5000 g for 10 min. The precipitate was then resuspended in 10 ml of 30 mM MOPS, 0.5 mM TCEP, 10 mM imidazole, pH 7.20. Cells were disrupted by sonication for 4 min at 30 % power. The cell lysate was separated from the cells by centrifugation at 18000*g* for 10 min. The protein was then bound to 500 μl of Ni-NTA resin (1:1 suspension) for 1 h at 4°C. After washing the resin 3 times with 5 ml of 30 mM MOPS, 0.5 mM TCEP, 10 mM imidazole, pH 7.20, we performed protein elution in 400 μl in 400 mM imidazole, 30 mM MOPS, 0.5 mM TCEP, pH 7.20 buffer. Proteins were dialyzed first at 4°C for 24 h opposite 1 L of 30 mM MOPS, 0.5 mM TCEP, 100 μM NTA, pH 7.20 buffer, and then 24 h at 4°C opposite 1 L of 30 mM MOPS, 0.5 mM TCEP, pH 7.20 buffer.

To determine the values of dissociation constants (K_d) with mercury ions, green fluorescence of the sensor (0.5 μM final concentration) was recorded after incubation at room temperature for 20–30 min in buffers of 50 mM Tris-HCl, 100 mM NaCl, 100 mM NaCl, 1 mM MgCl2, 10 mM NTA, pH 7. 2 and buffers of 50 mM Tris-HCl, 100 mM NaCl, 1 mM MgCl2, 1 mM MgCl2, 10 mM Hg-NTA, pH 7.2, mixed in ratios of 10:0, 199999:1, 99999:1, 19999:1, 9999:1, 1999:1, 999:1, 999:1, 199:1, 99:1, 9:1, 8:2, 7:3, 6:4, 5:5, 4:6, 3:7, 2:8, 1:9, and 0:10 (NTA is nitrilotriacetic acid). Free mercury ion concentration was calculated using the formula: $[Hg^{2+}]_{free} = K_d * [HgNTA]/[NTA]$, where K_d (HgNTA) = $2.51*10^{-15}$ M. For the ratio [HgNTA]:[NTA] = 10:0, we used another equation: $[Hg^{2+}]_{free} = \sqrt{K_d * [HgNTA]}$, where K_d (HgNTA) = $2.51*10^{-15}$ M. Kd values and Hill coefficients for mercury ion binding by sensors were calculated by nonlinear regression of experimental points by the Hill equation: $I = I_{max}\frac{[Hg^{2+}]^n}{K_d^n+[Hg^{2+}]^n}$, where I is the fluorescence intensity at a particular mercury concentration, and I_{max} is the fluorescence intensity at saturating mercury ion concentrations.

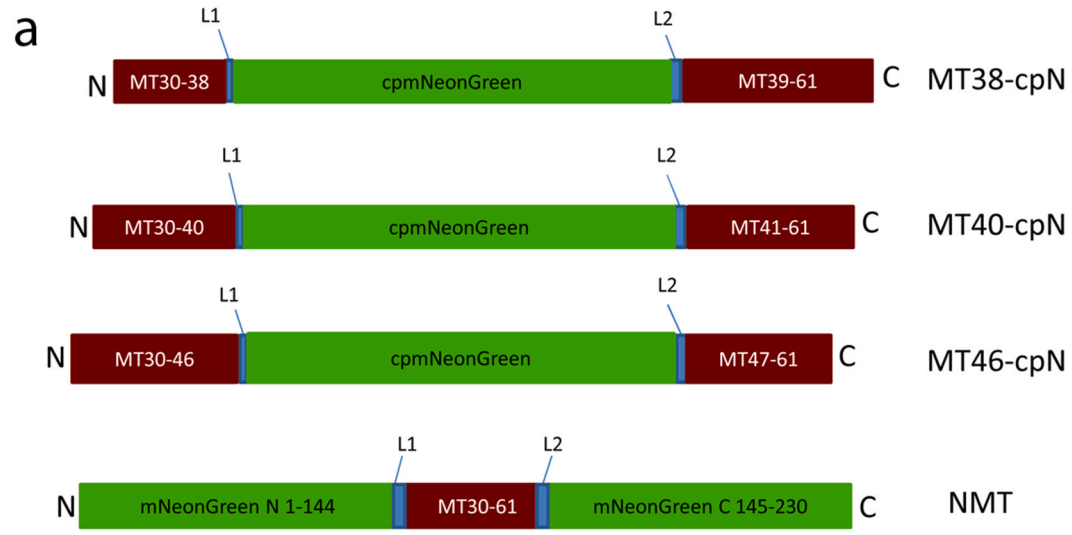

b

```
                1       10        20        30        40        50        60
                |       |         |         |         |         |         |
Library    MVSKGEEENMASLPATHELHIFGSINGIDFDMVGQGTGNPNDGYEELNLKSTMGDLQFSP
NMT        MVSKGEEENMASLPATHELHIFGSINGIDFDMVGQGTGNPNDGYEELNLKSTMGDLQFSP

               61        70        80        90       100       110       120
                |        |         |         |         |         |         |
Library    WILVPHIGYGFHQYLPYPDGMSPFQAAMVDGSGYQVHRTMQFEDGASLTVNYRYTYEGSH
NMT        WILVPHIGYGFHQYLPYPDGMSPFQAAMVDGSGYQVHRTMQFEDGASLTVNYRYTYGGSH

              121       130       140       150       160       170       180
                |       |         |         |         |         |         |
Library    IKGEAQVEGTGFPADGPVMTNSLTAXXXKSCCSCCPVGCAKCSQGCICKEASDKCSCCAX
NMT        IKGEAQVEGTGFPADGPVMTNSLTADTLKSSCSCCPVGCVKCSQGCICKEASDKCSCCAL

              181       190       200       210       220       230       240
                |       |         |         |         |         |         |
Library    XXADWCVSKKTCPNDKTIVSTFKWAFITDNGKRYRSTARTTYTFAKPMAANYLKNQPMYV
NMT        VSADWCVSKKTCPNDKTIVSTFKWAFITDNGKRYRSTARTTYTFAKPMAANYLKNQPMYV

              241       250       260       270
                |       |         |         |
Library    FRKTELKHSKTELNFKEWQKAFTDVMGMDELYK
NMT        FRKTELKHFKTELNFKEWQKAFTDVMGMDELYK
```

Fig. 1. Structure of the initial indicator libraries and amino acid sequence alignment of the initial library with randomized linkers and the final NMT mercury indicator. (a) MT, linkers, and cpmNeonGreen (or mNeonGreen parts) are shown in brown, blue, and green, respectively. In MT38-cpN, MT40-cpN and NT46-cpN L1 = XX, L2 = XXX; in NMT L1 = XXX, L2 = XXX. (b) Residues from fluorescent part buried in β-can are highlighted with green. Residues that are forming chromophore are underlined. Mutations in NMT related to the original library are highlighted in red. Linkers between fluorescent and mercury-binding parts are highlighted in blue. (For interpretation of the references to colour in this figure legend, the reader is referred to the Web version of this article.)

To determine the values of dissociation constants (Kd) with cadmium ions, green fluorescence of the sensor (0.5 μM final concentration) was recorded after incubation at room temperature for 20–30 min in buffers 50 MM Tris-HCl, 100 mM NaCl, 1 mM $MgCl_2$, 10 mM NTA, pH 7.2 and 50 MM Tris-HCl, 100 mM NaCl, 1 mM $MgCl_2$, 10 mM Cd-NTA, pH 7.2, mixed in ratios of 10:0, 9999:1, 1999:1, 999:1, 199:1, 99:1, 49:1, 32:1, 19:1, 13:1, 11.5:1, 9:1, 5:5 и 0:10. Free cadmium ion concentration was calculated using the formula: $[Cd^{2+}]_{free} = K_d*[CdNTA]/[NTA]$, where K_d (CdNTA) = $2.88*10^{-10}$ M. For the ratio [CdNTA]:[NTA] = 10:0, we used another equation: $\left[Cd^{2+}\right]_{free} = \sqrt{K_d * [CdNTA]}$, where K_d (CdNTA) = $2.88*10^{-10}$ M. K_d values and Hill coefficients for cadmium ion binding by sensors were calculated by nonlinear regression of experimental points by the Hill equation: $I = I_{max}\frac{\left[Cd^{2+}\right]^n}{K_d^n+\left[Cd^{2+}\right]^n}$, where I is the fluorescence intensity at a particular cadmium concentration, and I_{max} is the fluorescence intensity at saturating cadmium ion concentrations.

To test the selectivity of NMT sensor to different metal ions, fluorescence of purified protein (0.5 μM final concentration) incubated at room temperature for 5–10 min in buffer 50 mM Tris-HCl, 100 mM NaCl, 1 mM MgCl2, 10 mM Mt-NTA (where Mt is Sr, Mg, Cd, Pb, Ni, Zn, K, Mn, Ca, Ce, Fe, Cu or Hg) was compared with the fluorescence of protein in 50 mM Tris-HCl, 100 mM NaCl, 1 mM MgCl2, 10 mM NTA buffer. Green fluorescence (488/12 nm and 535/12 nm) was recorded on a plate reader. The values of ΔF/F were calculated according to the formula: $\Delta F/F = (I_{Mt\text{-}NTA}\text{-}I_{back1})/(I_{NTA}\text{-}I_{back2})\text{-}1$ и $\Delta F/F = -[(I_{NTA}\text{-}I_{back1})/(I_{Mt\text{-}NTA}\text{-}I_{back2})\text{-}1]$ for directed and inverted phenotypes respectively.

2.4. Statistical processing of the results

Figures show the mean values ± standard error.

2.5. Cell culture and transfection

HeLa Kyoto cells were maintained in Dulbecco's Modified Eagle Medium (DMEM) (GIBCO) supplemented with 10 % fetal bovine serum (FBS) (Sigma), 2 mM GlutaMax-I (GIBCO), 50 U/ml penicillin, and 50 μg/ml streptomycin (GIBCO). Plasmids for transfection were prepared using a Plasmid Miniprep purification kit (Evrogen, Russia). Transfection was performed using TurboFectTM (Thermo Fisher Scientific, USA) according to the manufacturer's protocol.

2.6. Mammalian live-cell imaging

HeLa Kyoto cell cultures were imaged 48 h after transfection equipped with an inverted Nikon Eclipse Ti microscope, a 75 W mercury-xenon lamp (Hamamatsu, Japan), a 60 × oil immersion objective (Nikon, Japan), a 16-bit QuantEM 512SC electron-multiplying CCD (Photometrics, USA), and a cage incubator (Okolab, Italy). For time-lapse imaging experiments, cells were visualized before and after the addition of 2.5 μM ionomycin, and 0.01, 0.1, 0.5, 1 or 10 mM Hg-NTA to induce fluorescence signal for Hg^{2+}-bound indicators.

3. Results

3.1. Development of NMT sensor

To develop an indicator for the detection of mercury ions, we chose to employ the cysteine-rich domain of metallothionein II (MT-II) from rat liver as a sensing domain [10]. The metallothionein isoform II from rat liver is composed of 61 amino acids, including 20 cysteines [11]. This protein consists of two domains: residues 1 to 29 (denoted β domain, and having 9 cysteines) and residues 30 to 61 (denoted α domain, with 11 cysteines) [12]. The α domain can bind four ions of heavy metals cooperatively [13]. First, we *de novo* synthesized the α domain of MT II from custom oligonucleotides and generated libraries with the randomized linkers, which were subsequently expressed and analyzed on crude bacterial extracts (Fig. 1a). We applied two molecular design strategies to generate indicator prototypes. First, a circularly permutated version of the mNeonGreen protein (cpmNeonGreen) was inserted into three different sites of the MT II α domain in loops near cysteine residues after amino acids 38, 40 and 46 (MT38-cpN, MT40-cpN and MT46-cpN). cpmNeonGreen was taken from a calcium indicator variant of NCaMP19-11 previously designed in our laboratory (unpublished data). The amino acids in the linkers (L1 = XX, L2 = XXX) between the MT II α domain and cpmNeonGreen proteins were randomized using site-directed mutagenesis (Fig. 1a). Second, we swapped the calcium-binding domain in the NCaMP7 calcium indicator with the MT II α domain [14]. The amino acids in the linkers (L1 = XXX, L2 = XXX) between the MT II α domain and mNeonGreen parts were varied (Fig. 1a).

For each bacterial library, the brightest colonies (typically 2–3 colonies per plate) were selected from about 20,000 colonies on Petri dishes, and the fluorescence response of the selected mutants to the addition of 5 nM of mercury ions was further tested on bacterial lysates in a 96-well format using a fluorescent plate reader. As a result of screening MT38-cpN, MT40-cpN, MT46-cpN, and NMT libraries, we obtained the best clone with a 1.9-fold negative fluorescence response for the NMT library. The responses were lower for other MT38-cpN, MT40-cpN, and MT46-cpN libraries, and we did not proceed with their optimization further.

The best clone was chosen as a template for several additional rounds of random mutagenesis of the entire biosensors' gene. The generated random libraries with a mutation rate of 1–3 base pairs per gene were screened as described above for libraries with

randomized amino acid linkers. We carried out 5 rounds of random mutagenesis and selected a variant characterized by a 3.5-fold fluorescence response (1.8-fold larger compared to the original precursor). Alignment of the amino acid sequence of NMT with the original rational library revealed that in addition to six mutations in the linkers, the sensors contained four additional mutations, two in the fluorescent part and two in the MT II part (Fig. 1b). In conclusion, swapping the calcium-binding domain in the NCaMP7 biosensor with the α domain of MT II was a successful approach to engineering a fluorescent mercury indicator with a negative fluorescence response.

3.2. Characterization of the specificity and the spectral and biophysical properties of the NMT indicator in vitro

First, we characterized the specificity of the NMT indicator to different metal ions, including heavy metals, namely Hg^{2+}, Cd^{2+}, Fe^{3+}, Cu^{2+}, Mn^{2+}, Ni^{2+}, Pb^{2+}, Zn^{2+}, Ce^{3+}, and physiologically important alkaline earth and alkali metals, namely Sr^{2+}, Ca^{2+}, Mg^{2+}, and K^{+} in physiological solution at constant ionic strength. We chose to use the concentration of the Mt-NTA (where Mt is metal, NTA is nitrilotriacetic acid) at 10 mM, which corresponds to the free metal ion concentration from 1 nM for Fe^{3+} to 186 μM for Mg^{2+}. In the case of K^{+} ions, the concentration was 10 mM because it did not form a complex with NTA. The negative fluorescence response of the NMT indicator was observed with the addition of mercury, cadmium, iron, and copper ions (Fig. 2a). The most significant fluorescence changes of −3.2-fold were detected in the presence of mercury ions, which elicited a double fluorescence change than that of cadmium ions (−1.6-fold for Cd^{2+}) and 4.3- and 9.7-fold fluorescence changes than those for iron (−0.75-fold) and copper (−0.32-fold) ions, respectively, indicating its higher sensitivity to mercury ions. In turn, the NMT indicator demonstrated either no response or a low positive response to the addition of other tested metal cations (the positive response was 2.3–29-fold lower than the negative response to mercury ions). Hence, the NMT indicator showed pronounced selectivity for mercury ions over other metal cations, indicating its potential as an optical molecular probe for detecting Hg^{2+} in various environmental and biological samples.

Then, we proceeded with the characterization of the spectral and biophysical properties of the NMT indicator purified from *E. coli* bacteria in the mercury-bound state. It exhibited absorption/excitation/emission maxima at 506/508/521 nm, respectively (Fig. 2b and Table 1). The molecular brightness, defined as the product of the extinction coefficient (determined by the alkaline denaturation method) by the quantum yield, was 166 % or 1.7-fold higher than that for the meGFP protein, the standard in the field of FPs (Table 1).

Next, we compared the affinity of the NMT indicator to mercury and cadmium ions. Titration of the NMT indicator with mercury and cadmium ions revealed the K_d values of 0.50 ± 0.05 aM and 289 ± 112 fM, respectively (Fig. 2c). Correspondingly, affinity to mercury ions is 578,000-fold higher than to cadmium ions. In addition, the NMT indicator binds more cooperatively with mercury ions than cadmium ions because the Hill coefficient values for mercury and cadmium ions are 0.93 ± 0.07 and 0.40 ± 0.06, respectively (Table 1). The maximally achievable ΔF/F contrast for mercury ion binding exceeds that for cadmium ion binding by a factor of 3.3 (−5.0 ± 0.1 and −1.5 ± 0.2 for mercury and cadmium ions, respectively; Table 1). Hence, the NMT indicator is specific to mercury ions in terms of better affinity, contrast, and binding cooperativity.

Thus, we have evaluated the selectivity of the NMT indicator to different metal ions and demonstrated its high sensitivity and specificity to mercury ions. Also, we characterized the spectral properties of the NMT indicator, its molecular brightness, affinity, and dynamic range.

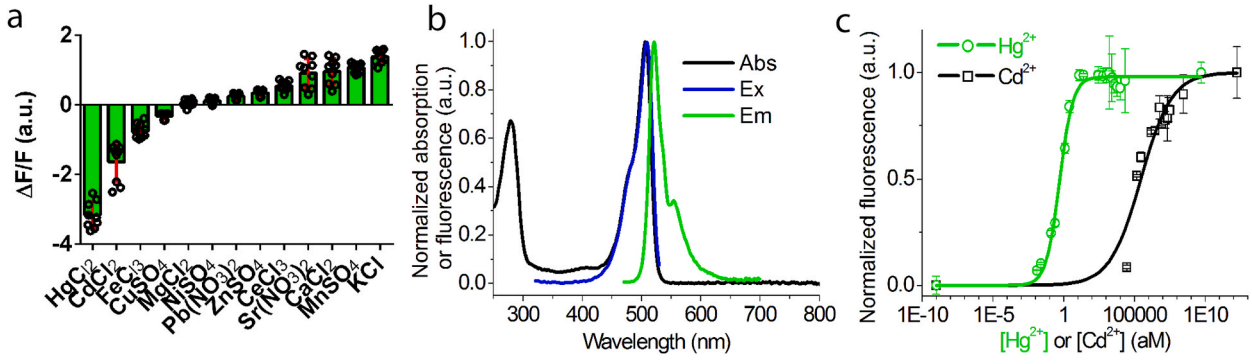

Fig. 2. Physicochemical and spectral properties of the NMT indicator in solution. (a) Selectivity of the NMT indicator to different metal ions. The fluorescence of proteins incubated at room temperature in buffer B: 50 mM Tris-HCl, 100 mM NaCl, 100 mM NaCl, 1 mM $MgCl_2$, 10 mM Mt-NTA, pH 7.2 (where Mt is Sr, Mg, Cd, Fe, Cu, Pb, Ni, Zn, K, Mn, Ca, Ce, or Hg; NTA is nitrilotriacetic acid) was compared with the fluorescence of proteins in buffer A: 50 mM Tris-HCl, 100 mM NaCl, 1 mM $MgCl_2$, 10 mM NTA, pH 7.2. ΔF/F in the presence of all metal ions was statistically different from ΔF/F in the presence of Hg^{2+}: $p < 0.0001$, ****. (b) Absorption, excitation and fluorescence spectra in 30 mM MOPS, 0.5 mM TCEP, pH 7.20 buffer. (c) Equilibrium binding curves of mercury or cadmium ions by the NMT indicator. Buffers A and B (0 mM Tris-HCl, 100 mM NaCl, 100 mM NaCl, 1 mM $MgCl_2$, 10 mM Hg-NTA, pH 7.2) were mixed in different ratios to vary the concentration of free mercury ions in the range of 0–5 nM. Buffers A and C (50 mM Tris-HCl, 100 mM NaCl, 1 mM $MgCl_2$, 10 mM Cd-NTA, pH 7.2) were mixed in different ratios to vary the concentration of free cadmium ions in the range of 0–1700 nM. Normalized fluorescence (Fnorm) was calculated as Fnorm = 1-(F-Fmin)/(Fmax-Fmin), where F, Fmax and Fmin are current, maximal and minimal fluorescence values respectively.

Table 1
Properties of the purified NMT indicator in solution.

		NMT	eGFP205C [7]	IFP [8]
Abs/Ex/Em Maxima, nm		506/508/521	~400/510	684/708
Exctinction coefficient, $mM^{-1}cm^{-1}$ [a]		89 ± 2	ND	92
Quantum yield [b]		0.73 ± 0.06	ND	0.07
Brightness vs meGFP, % [c]		166	ND	16
ΔF/F		5.0 ± 0.1	~0.3–1.3	>20
ΔF/F in cytosol of HeLa cells		5.9 ± 1.1	ND	4
K_d [d]	**Hg^{2+}**	0.50 ± 0.05 aM [0.93 ± 0.07]	~100 nM	150 nM or 2.3 μM
	Hg^{2+} in HeLa	293 ± 3 aM [1.89 ± 0.04]	ND	ND
	Cd^{2+}	287600 ± 111780 aM [0.40 ± 0.06]	ND	ND

ND, not determined.

[a] Extinction coefficients were determined in 1 M NaOH solution, assuming the absorption of the GFP chromophore under these conditions to be 44,000 $M^{-1}cm^{-1}$.

[b] Quantum yield was determined at an excitation light wavelength of 470 nm, relative to meGFP with quantum yield of 0.70.

[c] Brightness was determined as the product of quantum yield by extinction coefficient normalized to meGFP brightness equal to 100 %, assuming that the quantum yield and extinction coefficient for meGFP are 0.70 and 56 $mM^{-1}cm^{-1}$.

[d] Hill coefficient is indicated in square brackets.

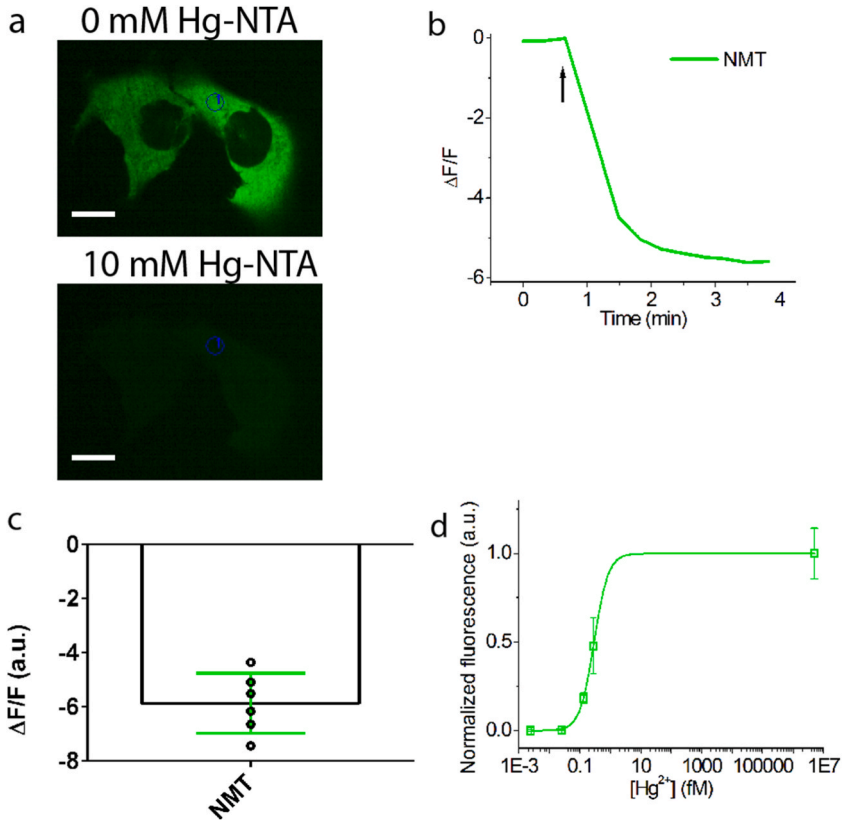

Fig. 3. Visualization of mercury ion concentration changes in HeLa cells with the NMT indicator using confocal fluorescence microscopy. (a) Confocal images of HeLa cells expressing NES-NMT before and after addition of 2.5 μM ionomycin and 10 mM HgNTA, 5 mM Tris-HCl, pH 7.40. Scale bar, 10 μm. (b) Time dependence of the ΔF/F green fluorescence change in the indicated region of the cell cytosol before and after addition of 10 mM Hg-NTA and 2.5 μM ionomycin at the time indicated by the arrow. (c) Averaged ΔF/F response of the NMT indicator in the cytosol of HeLa cells to the addition of 10 mM Hg-NTA and 2.5 μM ionomycin calculated from 2 cultures, 6 cells. (d) Titration of the NMT indicator expressed in the cytosol of HeLa cells with 0.01 mM Hg^{2+}-10mM NTA, 0.1 mM Hg^{2+}-10mM NTA, 0.5 mM Hg^{2+}-10mM NTA, 1 mM Hg^{2+}-10mM NTA and 10 mM Hg^{2+}-10mM NTA. The curve was plotted based on data from 5 cultures, 50 cells. Normalized fluorescence (Fnorm) was calculated as Fnorm = 1-(F-Fmin)/(Fmax-Fmin), where F, Fmax and Fmin are current, maximal and minimal fluorescence values respectively. (For interpretation of the references to colour in this figure legend, the reader is referred to the Web version of this article.)

3.3. Properties of NMT indicator in the cytosol of mammalian cells

To characterize the properties of the NMT indicator in mammalian cells, we transiently expressed the NMT indicator in the cytosol of HeLa Kyoto cells and visualized its response to the addition of the mercury ions. We transiently transfected HeLa Kyoto cells with pAAV-CAG-NES-NMT plasmid (NES stands for nuclei-exclusion signal). 48 h after transfection, we observed bright green fluorescence of the NMT indicator, which was evenly distributed in the cytosol of the cells, using confocal fluorescence microscopy (Fig. 3a). To check the cytotoxicity of the NMT indicator, we expressed the NMT indicator and GFP in two independent cultures each (about $3–5*10^5$ cells per ml). In addition, the transfection reagent was added to two cultures without DNA. Using staining with the trypan blue dye, we showed that cultures with the expressed NMT indicator, GFP, and with the transfection reagent contained 97 ± 1, 80 ± 24, and 73 ± 4 % of live cells, respectively. Hence, the NMT indicator is not cytotoxic for cells.

Then, we visualized changes in mercury ion concentration in the cytosol with addition to cells of 2.5 μM ionomycin and various concentrations of HgNTA (corresponding to 2.5 aM - 5 nM concentration of free mercury ions). We observed a decrease in green fluorescence of the NMT indicator (Fig. 3a and b) with the maximal averaged ΔF/F response equal to -5.9 ± 1.1 (Fig. 3c) and the K_d value of 0.29 ± 0.01 fM (Fig. 3d). Since the K_d value in solution is about 600-fold less than in mammalian cells, we can suggest that there is a gradient between the extracellular and intracellular concentration of mercury ion and 600-fold less mercury ions enter the cell. Similarly, an approximately 500-fold reduction in hydrogen peroxide concentration across the plasma membrane compared to the extracellular concentration was previously found [15]. Therefore, the NMT indicator can be used to monitor changes in the concentration of mercury ions in the cytosol of mammalian cells.

4. Discussion

In this paper, we describe the development of a novel green fluorescent NMT indicator for mercury ions. It was engineered by inserting the cysteine-rich metallothionein II domain into mNeonGreen bright green FP followed by a variation of linkers and directed molecular evolution. The NMT indicator has excellent properties both in vitro and in mammalian cells. The NMT indicator exhibited a 1.7-fold increase in brightness compared to the eGFP standard green FP and responded with extremely high sensitivity and specificity to mercury ions by the decrease of green fluorescence with a 5.0-fold fluorescence response. In addition, the NMT indicator robustly detected even tenths of femtomolar concentration of mercury ions in the cytosol of mammalian cells, demonstrating a 5.9-fold ΔF/F fluorescence response.

Previously two biosensors, eGFP205C [7] and IFP [8], for detection of mercury ions were published. The NMT indicator outperforms these sensors in sensitivity because its affinity to mercury ions is lower than affinities of eGFP205C and IFP by a factor of about 10^{11}. Also, the fluorescence response of the NMT indicator to mercury ions is 4-17-fold higher than that of eGFP205C. Moreover, the molecular brightness of eGFP205C and its behavior in mammalian cells have not been determined [7]. Compared to the IFP sensor, the molecular brightness of the NMT indicator is 10-fold higher [8]. In addition, the reaction of IFP with mercury ions depends on the presence of the biliverdin cofactor. There is no binding of IFP with mercury ions and no change in IFP fluorescence if biliverdin is added to IFP before mercury ions. On the contrary, the NMT fluorescence does not require the presence of any cofactors and its reaction with mercury ions has no such limitations.

We can suggest the mechanism of molecular interactions of the mercury ions with the NMT indicator. It is known that the α-domain of the MTII (which is a part of the NMT indicator) contains eleven cysteine residues and can bind four metal ions [10]. We think that the NMT indicator binds four mercury ions, and each of them is tetrahedrally coordinated by four thiols of cysteines. Mercury ion binding can lead to a change in the conformation of the mercury-binding part and affect the chromophore in the fluorescent part, resulting in a decrease in green fluorescence.

5. Conclusion

Here, we engineered the NMT green genetically encoded mercury indicator that is superior to those developed previously in terms of higher affinity, brightness, fluorescence response, and cofactor independence.

Data availability statement

Source files for the figures are available at FigShare (https://doi.org/10.6084/m9.figshare.25996654). Full length sequences of the generated plasmids are available from WeKwikGene (https://wekwikgene.wllsb.edu.cn/) with the following accession codes: pBAD-HisB-Sumo-NMT #0000575; pAAV-*Asc*I-CAG-NES-NMT #0000576.

CRediT authorship contribution statement

Oksana M. Subach: Writing – review & editing, Writing – original draft, Visualization, Validation, Investigation, Formal analysis, Data curation, Conceptualization. **Kiryl D. Piatkevich:** Writing – review & editing, Methodology, Funding acquisition, Formal analysis, Conceptualization. **Fedor V. Subach:** Writing – review & editing, Writing – original draft, Visualization, Validation, Supervision, Resources, Project administration, Methodology, Investigation, Funding acquisition, Formal analysis, Data curation, Conceptualization.

Declaration of competing interest

The authors declare that they have no known competing financial interests or personal relationships that could have appeared to influence the work reported in this paper.

Acknowledgments

The work was carried out within the state assignment of the National Research Center "Kurchatov Institute" (developing the NMT indicator); by the Ministry of Science and Higher Education of the Russian Federation for the development of the Kurchatov Center for Genome Research 075-15-2019-1659 (protein purification), by start-up funding from the Foundation of Westlake University, Westlake Laboratory of Life Sciences and Biomedicine, National Natural Science Foundation of China grants 32050410298 and 32171093; and 'Pioneer' and 'Leading Goose' R&D Program of Zhejiang 2024SSYS0031 to K.D.P (characterization of NMT in mammalian cells). The work was also supported by the Resource Centers department of the National Research Center Kurchatov Institute (imaging of bacteria cells).

Appendix A. Supplementary data

Supplementary data to this article can be found online at https://doi.org/10.1016/j.heliyon.2024.e32814.

References

[1] L.A. Malik, A.B, A. Qureashi, A.H. Pandith, Detection and removal of heavy metal ions: a review, Environ. Chem. Lett. 17 (2019) 1495–1521, https://doi.org/10.1007/s10311-019-00891-z.
[2] H. Ali, E. Khan, What are heavy metals? Long-standing controversy over the scientific use of the term 'heavy metals' – proposal of a comprehensive definition, Toxicol. Environ. Chem. 100 (2018) 6–19, https://doi.org/10.1080/02772248.2017.1413652.
[3] M.R. Slobodian, J.D. Petahtegoose, A.L. Wallis, D.C. Levesque, T.J.S. Merritt, The effects of essential and non-essential metal toxicity in the Drosophila melanogaster insect model: a review, Toxics 9 (2021), https://doi.org/10.3390/toxics9100269.
[4] M. Balali-Mood, K. Naseri, Z. Tahergorabi, M.R. Khazdair, M. Sadeghi, Toxic mechanisms of five heavy metals: mercury, lead, chromium, cadmium, and arsenic, Front. Pharmacol. 12 (2021) 643972, https://doi.org/10.3389/fphar.2021.643972.
[5] N. Soleja, O. Manzoor, P. Khan, M. Mohsin, Engineering genetically encoded FRET-based nanosensors for real time display of arsenic (As(3+)) dynamics in living cells, Sci. Rep. 9 (2019) 11240, https://doi.org/10.1038/s41598-019-47682-8.
[6] J.L. Vinkenborg, S.M. van Duijnhoven, M. Merkx, Reengineering of a fluorescent zinc sensor protein yields the first genetically encoded cadmium probe, Chem. Commun. 47 (2011) 11879–11881, https://doi.org/10.1039/c1cc14944j.
[7] R.R. Chapleau, R. Blomberg, P.C. Ford, M. Sagermann, Design of a highly specific and noninvasive biosensor suitable for real-time in vivo imaging of mercury (II) uptake, Protein Sci. : a publication of the Protein Society 17 (2008) 614–622, https://doi.org/10.1110/ps.073358908.
[8] Z. Gu, M. Zhao, Y. Sheng, L.A. Bentolila, Y. Tang, Detection of mercury ion by infrared fluorescent protein and its hydrogel-based paper assay, Anal. Chem. 83 (2011) 2324–2329, https://doi.org/10.1021/ac103236g.
[9] S.N. Ho, H.D. Hunt, R.M. Horton, J.K. Pullen, L.R. Pease, Site-directed mutagenesis by overlap extension using the polymerase chain reaction, Gene 77 (1989) 51–59, https://doi.org/10.1016/0378-1119(89)90358-2.
[10] W.F. Furey, A.H. Robbins, L.L. Clancy, D.R. Winge, B.C. Wang, C.D. Stout, Crystal structure of Cd,Zn metallothionein, Science 231 (1986) 704–710, https://doi.org/10.1126/science.3945804.
[11] D.R. Winge, K.B. Nielson, R.D. Zeikus, W.R. Gray, Structural characterization of the isoforms of neonatal and adult rat liver metallothionein, J. Biol. Chem. 259 (1984) 11419–11425, doi.org/.
[12] D.R. Winge, K.A. Miklossy, Domain nature of metallothionein, J. Biol. Chem. 257 (1982) 3471–3476, https://doi.org/10.1016/S0021-9258(18)34802-6.
[13] K.B. Nielson, D.R. Winge, Order of metal binding in metallothionein, J. Biol. Chem. 258 (1983) 13063–13069, doi.org/.
[14] O.M. Subach, V.P. Sotskov, V.V. Plusnin, A.M. Gruzdeva, N.V. Barykina, O.I. Ivashkina, K.V. Anokhin, A.Y. Nikolaeva, D.A. Korzhenevskiy, A.V. Vlaskina, et al., Novel genetically encoded bright positive calcium indicator NCaMP7 based on the mNeonGreen fluorescent protein, Int. J. Mol. Sci. 21 (2020), https://doi.org/10.3390/ijms21051644.
[15] Y.G. Ermakova, D.S. Bilan, M.E. Matlashov, N.M. Mishina, K.N. Markvicheva, O.M. Subach, F.V. Subach, I. Bogeski, M. Hoth, G. Enikolopov, et al., Red fluorescent genetically encoded indicator for intracellular hydrogen peroxide, Nat. Commun. 5 (2014) 5222, https://doi.org/10.1038/ncomms6222.